Clustering and viscosity in a shear flow of a particulate suspension

P. Raiskinmäki,[1] J. A. Åström,[1,2] M. Kataja,[1] M. Latva-Kokko,[1] A. Koponen,[1] A. Jäsberg,[1] A. Shakib-Manesh,[1] and J. Timonen[1]

[1]*Department of Physics, P.O. Box 35, FIN-40014 University of Jyväskylä, Finland*

[2]*Laboratory of Physics, P.O. Box 1100, FIN-02015 Helsinki University of Technology, Finland*

(Received 27 June 2003; published 17 December 2003)

A shear flow of particulate suspension is analyzed for the qualitative effect of particle clustering on viscosity using a simple kinetic clustering model and direct numerical simulations. The clusters formed in a Couette flow can be divided into rotating chainlike clusters and layers of particles at the channel walls. The size distribution of the rotating clusters is scale invariant in the small-cluster regime and decreases rapidly above a characteristic length scale that diverges at a jamming transition. The behavior of the suspension can qualitatively be divided into three regimes. For particle Reynolds number $\mathrm{Re_p} \lesssim 0.1$, viscosity is controlled by the characteristic cluster size deduced from the kinetic clustering model. For $\mathrm{Re_p} \sim 1$, clustering is maximal, but the simple kinetic model becomes inapplicable presumably due to onset of instabilities. In this transition regime viscosity begins to increase. For $\mathrm{Re_p} \gtrsim 10$, inertial effects become important, clusters begin to breakup, and suspension displays shear thickening. This phenomenon may be attributed to enhanced contribution of solid phase in the total shear stress.

DOI: 10.1103/PhysRevE.68.061403 PACS number(s): 83.80.Hj, 47.15.Pn, 83.60.Rs

I. INTRODUCTION

The dynamics of systems composed of solid particles suspended in a fluid are important in natural as well as technological processes. The flow of blood is just one example of an important (and complicated) suspension flow appearing in nature. Spreading of paint is another everyday example, also of shear flows of suspensions which typically appear in ''technological'' processes.

The behavior of a suspension strongly depends on the volume fraction of the solid particles, ϕ. In the limit of small ϕ and vanishing Reynolds number, the relative viscosity η_r, defined as the ratio of the viscosity of the suspension to that of the pure fluid, is well approximated by Einstein's formula [1]

$$\eta_r = 1 + 2.5\phi + O(\phi^2). \tag{1}$$

Close to the (random) dense packing limit, the effects of the fluid mostly vanish, η_r diverges, and suspension becomes a wet granular medium [2]. If cohesive forces exist between particles, the suspension may even transform into a solid [3].

For a nonzero ϕ, η_r also depends on the particle Reynolds number $\mathrm{Re_p}$ (see below). Experiments indicate [4] that, for low $\mathrm{Re_p}$, η_r decreases, and for $\mathrm{Re_p} \gtrsim 1$, η_r increases with increasing $\mathrm{Re_p}$ (shear rate). A qualitative explanation suggested [5] to this behavior is that, for very low $\mathrm{Re_p}$, suspended particles are randomly distributed due to Brownian motion. As the shear rate increases, hydrodynamic forces begin to organize particles in layers oriented perpendicular to the velocity gradient. This increasing ordering allows particles to move past each other without colliding and leads to the observed decrease of η_r, i.e., to shear thinning. Above a distinct value of $\mathrm{Re_p}$ near unity these layers seem to vanish. At this point a sudden increase of η_r, i.e., shear thickening, is observed [6]. Another qualitative explanation suggested to the strong shear thickening for $\mathrm{Re_p} > 1$ is enhanced clustering of particles [7,8]. Large clusters are assumed to provide efficient mechanisms for momentum transfer, and to thereby increase η_r. As the cluster size grows, the suspension approaches a jamming transition [9], and $\eta_r \propto (\phi - \phi_c)^{-\alpha}$ as $\phi \to \phi_c$. This form for η_r is similar to the semiempirical Krieger formula [10] for which $\alpha \approx 2$ and $\pi/6 \lesssim \phi_c \lesssim 0.74$ (in 2D $\alpha \approx 2$ and $\phi_c \approx \pi/4$), which is in good agreement with experimental results for low $\mathrm{Re_p}$. For higher $\mathrm{Re_p}$'s one would expect a similar divergence to occur, but with values for α and ϕ_c that may depend on $\mathrm{Re_p}$.

It has proved quite difficult to obtain conclusive experimental evidence to validate (or invalidate) the various microscopic mechanisms that have been suggested for the observed macroscopic behavior of liquid-particle suspensions. In this investigation we use a schematic clustering model together with numerical simulations to study the basic mechanisms underlying the shear thickening behavior of particulate suspensions, in a regime where Brownian motion and the associated shear thinning can be neglected. The clustering model introduced below is based on very generic arguments applicable in Couette flow. It yields a specific functional form for the cluster-size distribution and suggests a general dimensional relation for η_r. The model predictions are tested using direct numerical simulations. For simplicity, we use here a two-dimensional (2D) numerical solution. It can be argued, however, that most of the *qualitative* results thus obtained can be generalized to 3D flows.

The most important result is that at low Reynolds numbers a link is established between the well-known semiempirical Krieger formula for effective viscosity and the generic cluster-size distribution. This result explains, at least partially, the physical origin of the Krieger formula. Not very surprisingly, for higher Reynolds-number values inertial effects become increasingly important, and the generic clustering model gradually loses its validity.

II. CLUSTERING MODEL

We now consider general aspects of particle clustering in a low $\mathrm{Re_p}$ Couette flow. We ignore Brownian motion and

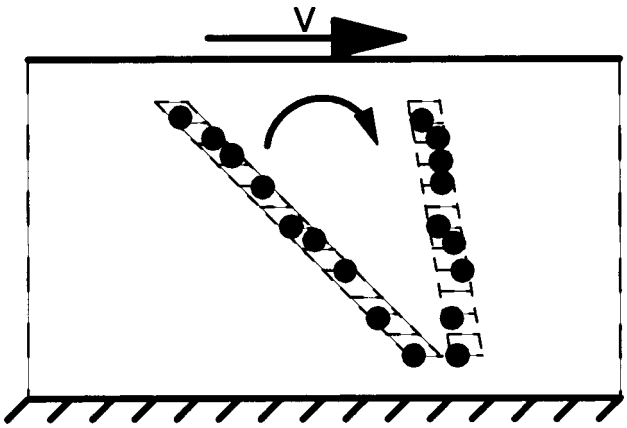

FIG. 1. Schematic presentation of the KCM model.

assume that particles can interact by elastic collisions and by hydrodynamic ''lubrication'' forces. For very low $\mathrm{Re_p}$'s the hydrodynamic forces acting on the particles are those of Stokes flow, and the particles move according to a linear (Newtonian) fluid-velocity profile, until they encounter another particle. As lubrication forces dominate the particle-particle interactions, these ''collisions'' are almost perfectly inelastic, and colliding particles will stay together for some time and form a ''cluster.'' These clusters will evolve in time and form a definite cluster-size distribution in a stationary flow.

Consider a part of the suspension located within a long and narrow tubular volume elements at a small angle across the shear cell, such that the flow velocity at the trailing end is higher than at the leading end of the element (Fig. 1). Initially the particle centers of mass are sparsely located and uncorrelated in the tube so that their density distribution is Poissonian. As this imaginary tube rotates in the shear velocity field, it will become broader and shorter. Particles therein will approach each other and begin to collide. If m particles come within a range of md, where d is the particle diameter, a cluster of size m will be formed. According to this kinetic clustering model (KCM), the cluster-size distribution $n(m)$ is then given by

$$n(m)=\frac{1}{m}\frac{(m\lambda)^m e^{-m\lambda}}{m!}, \tag{2}$$

where λ is the average number of particles in a unit length of the tube. Here, d is set to unity. The linear density λ can be related to the volume fraction ϕ of particles by $\lambda=\phi/\phi_c$, where ϕ_c is the volume fraction at maximum linear density. Using Stirling's formula for $m!$, we then find that

$$n(m)\propto m^{-1.5}\exp(-m/m_0), \tag{3}$$

where $m_0=1/[\phi/\phi_c-\ln(\phi/\phi_c)-1]$. The distribution Eq. (3) is scale invariant for $m\ll m_0$ and it decreases rapidly for $m>m_0$. The crossover cluster size m_0 diverges when ϕ reaches ϕ_c, which indicates that infinitely large clusters appear in the system in this limit. This divergence represents a jamming limit at which viscosity is also expected to diverge

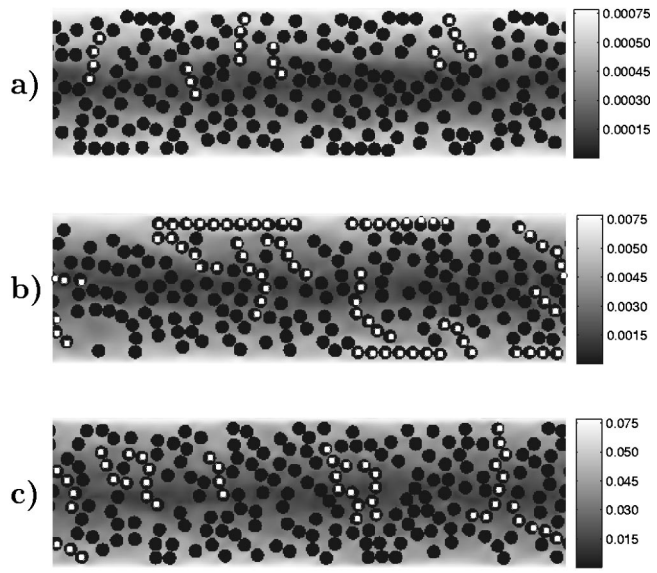

FIG. 2. (Color online) Snapshots of suspensions for $\mathrm{Re_p}=0.1$ (a), $\mathrm{Re_p}=1$ (b), and $\mathrm{Re_p}=10$ (c); $\phi=0.4$. A few clusters are indicated. The walls with distance 130 lu move in opposite directions creating a shear field. Fluid velocity is indicated by gray scale so that white indicates high velocity (in addition the color bar on the right indicates the velocity scale in lattice units).

[9]. Since m_0 is the only variable related to clustering, we would expect the relative viscosity in the Stoke's flow regime to be of the form

$$\eta_r=1+f(m_0), \tag{4}$$

in which 1 relates to the viscosity of the pure fluid, and f is an unknown (''scaling'') function that describes the part of the viscosity which originates from the clustered particles.

III. NUMERICAL MODEL

In order to test Eq. (3), and to extract f, we performed numerical simulations of liquid-particle suspension in a 2D shear flow. The numerical algorithm used here is that of the nine-link lattice-Boltzmann (LB) method [11–14]. It is based on solving a discretized Boltzmann equation for the fluid phase on a regular lattice. The solid particles move continuously in space and collide with each other and with bounding walls. Hydrodynamic interaction (momentum exchange) between the solid phase and the Newtonian fluid phase is taken into account by applying the no-slip boundary condition at the boundary nodes. The forces from this interaction and from the collisions determine the translation and rotation of the suspended solid particles according to Newtonian dynamics. Note that the LB method used here accounts for all hydrodynamic effects present in the Navier-Stokes equation, including viscous forces, pressure forces, and inertial effects. A more detailed description of the method can be found in Ref. [14] and our benchmarking results in Ref. [15].

The shear-flow condition was realized by placing the suspension between two walls separated by distance h (cf. Fig. 2), such that the walls moved with speed v_w in opposite directions. Periodic boundary conditions were imposed in the

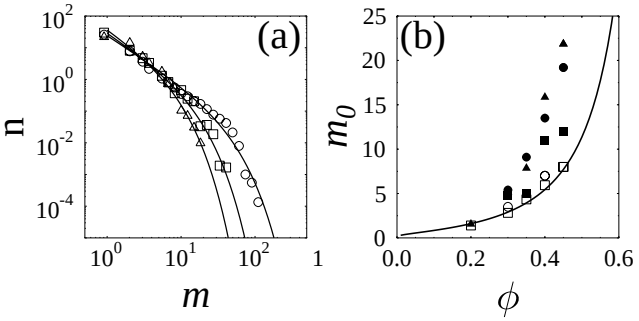

FIG. 3. (a) Cluster-size distributions for $\phi=0.4$: $\mathrm{Re_p}=0.01$ (△), $\mathrm{Re_p}=0.1$ (□), $\mathrm{Re_p}=1.0$ (○). The solid lines indicate the distributions predicted by KCM. (b) m_0 as a function of ϕ for $\mathrm{Re_p}=0.06$ (□),0.3 (■),0.8 (●),1.4 (▲); the channel width is $h=130$. For $\mathrm{Re_p}=0.06$ another channel width was also used, $h=260$(○). The solid line is the theoretical relation Eq. (6).

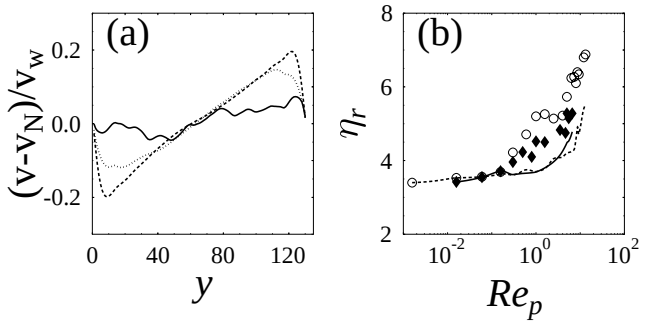

FIG. 4. (a) Difference of the simulated v and Newtonian v_N velocity profile, normalized by v_w as a function of distance from the lower wall, for $\mathrm{Re_p}=0.1$ (solid line), $\mathrm{Re_p}=1.0$ (dotted line), and $\mathrm{Re_p}=10.0$ (broken line). (b) Apparent and intrinsic viscosities as functions of $\mathrm{Re_p}$ for $h=130$ (broken line, ○) and $h=260$ (solid line, ♦), respectively.

flow direction. The density of the suspended particles was 2.5 times that of the carrier fluid, and no Brownian motion was implemented.

The volume fraction (area fraction) of the particles was varied between $\phi=0.20$ and $\phi=0.45$. These values are clearly above the regime in which Eq. (1) is valid, and below the jamming transition limit which for the 2D case considered here is that of a regular square lattice of spherical particles, i.e., $\phi_c=\pi/4$. In the used numerical method the kinematic viscosity of the carrier fluid is related to the LB relaxation parameter τ by $\nu=(2\tau-1)/6$. Here we used $\tau=0.55$ whereby $\nu=1/60$ [in lattice units (lu)]. The particle Reynolds number $\mathrm{Re_p}=\gamma d^2/\nu$, with $\gamma=2v_w/h$ the mean shear rate, was varied between 0.001 and 13. The size of the simulation grid was 130×450 lattice points and the particle diameter 12 lu. A few larger simulations with 260×900 grid size were performed in order to estimate the finite-size effects.

IV. RESULTS

Figure 2 shows snapshots of suspensions for particle Reynolds numbers $\mathrm{Re_p}=0.1$, 1, and 10. Some typical particle aggregates (clusters) are indicated in the figure. Clusters were identified such that the largest allowed distance between the nearest-neighbor particles within an aggregate was one lu. In accordance with the common view discussed above, two types of clusters with quite distinct characteristics indeed appear in the 2D flow. Near the moving walls, horizontal layers of particles can be found. These layers appear at a relatively low $\mathrm{Re_p}$ and their formation mechanism is most likely related to lateral hydrodynamic forces (lift forces) exerted on particles moving near a solid wall [16]. The dynamics of these layers is not studied here in more detail. In the interior of the flow channel, chainlike clusters form and rotate under the shear flow, much in accordance with the generic clustering model discussed above.

In the entire region covered by the present simulations the size distribution of the rotating clusters is indeed given by Eq. (3) as predicted by the KCM. This is demonstrated in Fig. 3(a). Thus, m_0 is the only parameter indicative of cluster size. In general the size distribution may, however, depend on both ϕ and $\mathrm{Re_p}$.

Given this basic result, we now proceed to seek the cluster-size parameter m_0, and η_r, in the form

$$m_0=m_0(\phi,\mathrm{Re_p}),\qquad \eta_r=\eta_r(\phi,\mathrm{Re_p}). \tag{5}$$

In particular, we test against numerical results the two additional explicit predictions of the KCM model, namely that η_r is a function of only m_0, and that m_0 is given in terms of the volume fraction of particles as

$$m_0=m_0^{KCM}(\phi)\equiv\left[\frac{\phi}{\phi_c}-\ln\left(\frac{\phi}{\phi_c}\right)-1\right]^{-1}. \tag{6}$$

The present numerical simulations show qualitatively different behavior in three distinct flow regimes: viscous regime for $\mathrm{Re_p}\lesssim0.1$, transition regime for $\mathrm{Re_p}\sim1$, and inertial regime for $\mathrm{Re_p}\gtrsim10$.

In the viscous regime there is no visible formation of particle layers near the walls and the average size of the rotating clusters is small as can be seen in e.g., Fig. 2(a). A comparison between Eq. (6) and simulation results reveals a close to perfect agreement in this region [Fig. 3(b)]. (For larger values of $\mathrm{Re_p}$, m_0 increases considerably.) The average velocity profile across the channel displays only small fluctuations around a Newtonian (straight) profile, as demonstrated in Fig. 4(a). This regime is thus that of laminar Stokes flow. We would consequently expect the effective viscosity to have little, if any, $\mathrm{Re_p}$ dependence. This is confirmed in Fig. 4(b). We can then proceed to extract the function f of Eq. (4). This can be done by plotting η_r-1 as a function of m_0. The result is shown in Fig. 5. For the lowest values of $\mathrm{Re_p}$ a linear function $f(m_0)\approx0.5m_0$ gives a reasonable fit to the simulation data. It is also worth noting that when this form of f is inserted in Eq. (4), the Krieger formula is found for ϕ/ϕ_c close to unity. For comparison, the Krieger formula $(1-\phi/\phi_c)^{-2}$ with $\phi=\phi(m_0)$ via Eq. (6) is also shown in Fig. 5(a). In the viscous regime we thus have $m_0=m_0^{KCM}(\phi)$, and

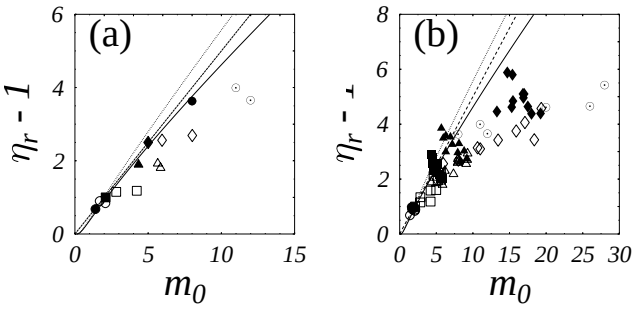

FIG. 5. (a) $\eta_r - 1$ as a function of m_0 for $\mathrm{Re_p} \leqslant 1$ and $\phi = 0.2$ (○),0.3 (□),0.35 (△),0.4 (◇),0.45(⊙). The filled symbols indicate $\mathrm{Re_p} = 0.06$. (b) $\mathrm{Re_p} \leqslant 13.0$. Filled symbols correspond to the inertial regime, wherein m_0 slightly decreases. The solid line and the dotted line indicate the results of Krieger formula with powers -1.8 and -2.0, respectively. The broken line is $1 + 0.5 m_0$.

$$\eta_r = \eta_r(m_0) \approx 1 + 0.5 m_0 \approx \left(1 - \frac{\phi}{\phi_c}\right)^{-2}, \tag{7}$$

which means that η_r depends only on m_0 given by the KCM model.

In the transition regime wall layers develop and reach their maximum average size. Also the size of the rotating clusters (i.e., m_0) grows considerably. Both these effects are visible in Fig. 2(b). However, m_0 is no longer given by Eq. (6) as can be seen from Fig. 3(b). Also η_r grows in this regime but not in proportion to the increase in m_0. In the transition regime

$$m_0 = m_0(\phi, \mathrm{Re_p}) > m_0^{KCM}(\phi),$$

$$\eta_r = \eta_r(m_0, \mathrm{Re_p}) < 1 + 0.5 m_0. \tag{8}$$

In this regime we thus have the general form of Eq. (5) without any reduction of dependencies. This means that the KCM model now fails, except for the form of the cluster-size distribution. The velocity profile deviates from the Newtonian one, and an S-shaped profile with higher shear close to the walls is developed [Fig. 4(a)]. Consequently, two different definitions of viscosity are possible: intrinsic viscosity, which is a bulk property calculated using the shear rate in the middle of the channel, and apparent viscosity calculated using the average shear rate (measurable but affected by the flow profile, i.e., boundary layers). The two viscosities are displayed in Fig. 4(b) for a few values of $\mathrm{Re_p}$.

Above $\mathrm{Re_p} \sim 10$ flow instabilities arise signifying an incipient inertial regime. In these conditions particle layers near the walls largely disappear. The typical cluster size inside the flow region also starts to decrease due to stronger velocity fluctuations. This is seen as a slight decrease of m_0 when compared to the transition regime [Fig. 5(b)]. The unreduced form of Eq. (5) is valid. The S shape of the velocity profile becomes more pronounced [Fig. 4(a)] and η_r increases rapidly with increasing $\mathrm{Re_p}$ [Fig. 4(b)]. Based on our earlier work [17], this shear thickening seems to be related to the enhanced relative contribution of the solid phase in the total shear stress. The increased particulate stress arises due to inertial effects resulting in enhanced fluid-particle interaction through pressure forces [18].

V. CONCLUSION

In conclusion, we used a generic KCM to study the basic mechanisms underlaying shear thickening of particulate suspensions in the regime where hydrodynamical forces dominate. We also performed direct numerical simulations of a 2D shear flow using the lattice-Boltzmann method. We expect the results obtained to be qualitatively valid also for 3D flows.

The cluster-size distribution of the suspended particles is scale invariant below an exponential cutoff [see Eq. (3)] in the regime covered by the present simulations. Three qualitatively different flow regimes were identified. In the viscous regime where the particle Reynolds number $\mathrm{Re_p} \lesssim 0.1$, chainlike clusters rotating in the shear field are comparatively small, and the relative viscosity η_r is a function of only the typical cluster size given by the KCM model. In this regime the KCM model can be linked to the Krieger formula via Eqs. (6) and (7). This suggests that the origin of the rather universal validity of Krieger formula at least partially finds its explanation in the general assumptions of the KCM model. In the transition regime $\mathrm{Re_p} \sim 1$, the size of the clusters grows considerably, but the typical size is no longer given by the KCM model. Also η_r begins to grow with $\mathrm{Re_p}$, but not in proportion to the growth of the cluster size. Inertia begins to take effect already in the transition regime, but especially in the third (inertial) regime where $\mathrm{Re_p} \gtrsim 10$. In the inertial regime flow becomes more unstable and there is no simple correlation between η_r and cluster size. The pronounced shear thickening in this regime seems to be related to enhanced relative contribution of the solid phase to the total shear stress in the suspension.

[1] A. Einstein, Ann. Phys. (Leipzig) **17**, 459 (1905); **19**, 271 (1906); **34**, 591 (1911).
[2] D. Hornbaker, R. Albert, I. Albert, A.L. Barabasi, and P. Schiffer, Nature (London) **387**, 6635 (1997).
[3] V. Trappe, V. Prasad, L. Cipeletti, P.N. Segre, and D.A. Weitz, Nature (London) **441**, 772 (2001).
[4] R.L. Hoffman, Trans. Soc. Rheol. **16**, 155 (1972).
[5] H.A. Barnes, J.F. Hutton, and K. Walters, *An Introduction to Rheology* (Elsevier, Amsterdam, 1993).
[6] D.I. Dratler, W.R. Schowalter, and R.L. Hoffman, J. Fluid Mech. **353**, 1 (1997).
[7] J.F. Brady and G. Bossis, J. Fluid Mech. **155**, 105 (1985).
[8] J.F. Brady and G. Bossis, Annu. Rev. Fluid Mech. **20**, 111 (1988).

[9] R.S. Farr, J.R. Melrose, and R.C. Ball, Phys. Rev. E **55**, 7203 (1997); S.F. Edwards and D.V. Grinev, *Jamming and Rheology: Constrained Dynamics on Microscopic and Macroscopic Scales*, edited by A.J. Liu and S.R. Nagel (Taylor & Francis, New York, 2001).
[10] I.M. Krieger and T.J. Dougherty, Trans. Soc. Rheol. **3**, 137 (1959); I.M. Krieger, Adv. Colloid Interface Sci. **3**, 111 (1972).
[11] A.J.C. Ladd, J. Fluid Mech. **271**, 311 (1994).
[12] A.J.C. Ladd and R. Verberg, J. Stat. Phys. **104**, 1191 (2001).
[13] C.K. Aidun and Y. Lu, J. Stat. Phys. **81**, 49 (1995).
[14] O. Behrend, Phys. Rev. E **52**, 1164 (1995).
[15] P. Raiskinmäki, A. Shakib-Manesh, A. Koponen, A. Jäsberg, M. Kataja, and J. Timonen, Comput. Phys. Commun. **129**, 185 (2000).
[16] A. Jäsberg, A. Koponen, M. Kataja, and J. Timonen, Comput. Phys. Commun. **129**, 196 (2000).
[17] A. Shakib-Manesh, P. Raiskinmäki, A. Koponen, M. Kataja, and J. Timonen, J. Stat. Phys. **107**, 67 (2002).
[18] P. Raiskinmäki *et al.* (unpublished).